

# Structure of cytochrome $c_{555}$ of *Chlorobium thiosulfatophilum*: Primitive low-potential cytochrome $c$

(protein evolution/heme proteins)

Z. R. KORSZUN AND F. R. SALEMME

Department of Chemistry, University of Arizona, Tucson, Arizona 85721

Communicated by H. E. Carter, September 27, 1977

**ABSTRACT** Cytochrome  $c_{555}$  is an 86-residue type  $c$  cytochrome derived from *Chlorobium thiosulfatophilum*, an obligately anaerobic green sulfur bacterium which is among the most primitive of living organisms. Here is presented a preliminary structural description of the cytochrome  $c_{555}$  molecule based on its crystallographic structure determination at 2.7-Å resolution by multiple isomorphous replacement methods. This structure is of interest not only because of its evolutionary significance but also because the cytochrome  $c_{555}$  molecule possesses an unusually low physiologic oxidoreduction potential ( $E_{m,7} = +145$  mV) compared with related members of the cytochrome  $c$  family. Consequently, determination of its structure may permit a direct assessment of the structural factors responsible for prosthetic group redox potential regulation in type  $c$  cytochromes.

The high-potential type  $c$  cytochromes comprise a functional molecular family of nearly universal species diversification. Typically, these heme-proteins are composed of a single polypeptide chain of 85-135 residues with a single covalently bound protoheme IX prosthetic group whose iron is axially ligated by a histidine imidazole nitrogen and a methionine sulfur atom (1, 2). Included are mitochondrial cytochromes  $c$ , the bacterial photosynthetic cytochromes  $c_2$ , *Paracoccus denitrificans*  $c_{555}$ , *Pseudomonas* cytochromes  $c_{551}$ , algal cytochromes  $f$ , and *Chlorobium* cytochromes  $c_{555}$ . All of these molecules share some degree of amino acid sequence homology although, in contrast to the extreme sequential conservatism manifest in the eukaryotic mitochondrial cytochromes  $c$ , there is considerable sequential diversity among the prokaryotic types (3). Nevertheless, they all appear to function similarly physiologically—i.e., they are generally peripheral membrane proteins serving as electron donors to the most oxidizing membrane-bound electron acceptor of the oxidative or photophosphorylating electron transport chain in which they function.

The presence of type  $c$  cytochrome in *Chlorobium thiosulfatophilum*, a green sulfur bacterium, was first reported by Kamen and Vernon (4). The principal basic soluble component, cytochrome  $c_{555}$ , has subsequently been studied in several laboratories (5-7) and has recently been sequenced (8). It is a protein of molecular weight 9030, having 86 amino acid residues and a single covalently bound protoheme IX.

The structure determination of this protein was undertaken for the following reasons. First, the obligately anaerobic green sulfur bacteria, which primarily utilize  $H_2S$  as a source of reducing electrons (9), are generally considered to be among the most primitive living organisms (Fig. 1). Second, cytochrome  $c_{555}$  of *C. thiosulfatophilum* possesses an unusually low standard oxidoreduction potential ( $E_{m,7} = +145$  mV) compared with the mitochondrial cytochromes  $c$  ( $\sim +260$  mV), the bac-

terial cytochromes  $c_2$  ( $\sim +320$  mV), the *Pseudomonas* cytochromes  $c_{551}$  ( $\sim +285$  mV), or the algal cytochromes  $f$  ( $\sim +370$  mV) (10). Third, *C. thiosulfatophilum*  $c_{555}$  has been shown to possess activity in the mitochondrial cytochrome  $c$  oxidase system while being unreactive with mitochondrial cytochrome  $c$  reductase (11, 12). This reactivity pattern contrasts with that exhibited by other prokaryotic cytochromes  $c$  and is the reverse of that observed for the bacterial photosynthetic cytochromes  $c_2$  which are readily reduced by mitochondrial cytochrome  $c$  reductase but react poorly with cytochrome oxidase (11, 12). In addition, it is notable that the reactivity of *C. thiosulfatophilum* cytochrome  $c_{555}$  with cytochrome oxidase does not appear to be directly related to the former molecule's low oxidoreduction potential, because it has been observed that the homologous cytochrome  $c_{555}$  of *Prosthecochloris aestuarii* ( $E_{m,7} = 103$  mV) shows no reactivity with mitochondrial cytochrome oxidase or reductase (12, 13). Consequently, it is hoped that a structural comparison of the *C. thiosulfatophilum*  $c_{555}$  molecule with other cytochromes  $c$  with different reactivities will aid in the elucidation of the structural characteristics that confer reactive specificity upon these molecules.

We here present a preliminary description of the conformation of cytochrome  $c_{555}$  based upon interpretation of an electron density map incorporating data to 2.7-Å resolution.

## METHODS

Cytochrome  $c_{555}$ , kindly provided by T. Meyer, R. Bartsch, and M. Cusanovich, was crystallized by layering 50  $\mu$ l of protein solution (50 mg/ml) over an equal volume of 65% saturated ammonium sulfate/0.1 M  $Mg(NO_3)_2$  in 6  $\times$  15 mm test tubes (13). Rod-shaped crystals were obtained in the orthorhombic space group  $P2_12_12_1$  with unit cell parameters of  $a = 48.3$  Å,  $b = 24.5$  Å,  $c = 60.1$  Å,  $V = 7.11 \times 10^4$  Å<sup>3</sup>.

Replicated data, including Bijvoet related reflections, were collected by using  $\theta$ - $\omega$  step scans in oxidized parent crystals and in  $UO_2(NO_3)_2$  (four sites),  $K_2HgI_4$  (four sites), and mersalyl (three sites) derivative crystals on a Picker FACS1 automatic diffractometer having a 560-W monochromated Cu source. Complete data sets were collected on single crystals, which generally showed about 15% loss in intensity of a set of periodically measured standard reflections by the end of the data collection to 2.7 Å ( $\sim 6500$  reflections). Background intensities were counted for approximately 10% of the reflection scan interval. Comparison of background intensities measured in this way with those computed by using an empirical  $2\theta$  scan technique (14) for all data sets suggested that the counted backgrounds were more accurate. Consequently, raw intensity data were corrected by using counted background values.

Intensity data were further corrected for crystal absorption (15, 16) and Lorentz and polarization effects prior to final scaling to compensate for radiation damage. Scaling R factors

The costs of publication of this article were defrayed in part by the payment of page charges. This article must therefore be hereby marked "advertisement" in accordance with 18 U. S. C. §1734 solely to indicate this fact.

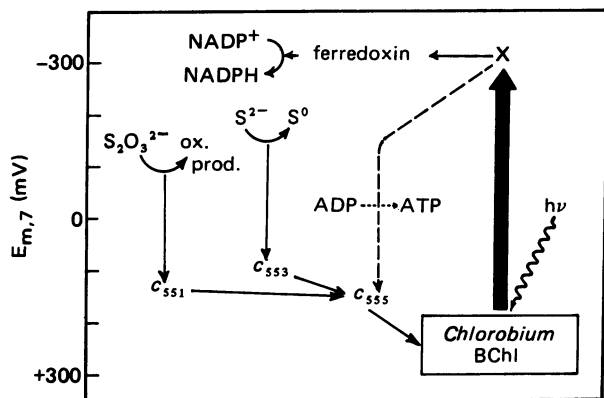


FIG. 1. Diagram of the electron transport chain of *C. thiosulfatophilum*, a green sulfur bacterium. Reducing electrons derived from thiosulfate or hydrogen sulfide are respectively funneled through cytochromes  $c_{551}$  or  $c_{553}$  to cytochrome  $c_{555}$  which subsequently reduces photooxidized bacteriochlorophyll (BChl). Cytochrome  $c_{555}$  may also function in the cyclic photophosphorylating chain of the organism (shown as dashed lines), in a manner similar to that of the cytochromes  $c_2$  of the purple nonsulfur bacteria (9).

between all replicated reflection intensities of a given data set were 3–5%.

Heavy atom sites were located by interpretation of heavy atom difference Patterson maps and were assigned to a common origin by utilizing calculated phases from one derivative to locate sites on heavy atom difference Fourier maps of consecutive derivatives.

Phases were refined by the usual method of minimizing  $\sum [K F_H(\text{obs}) - F_H(\text{calc})]^2$  in alternating cycles of phase calculation and refinement of heavy atom parameters. Anomalous dispersion effects were incorporated in the phase refinement process as described by Matthews (17). The final figure of merit to 2.7-Å resolution was 0.69.

Refined phases were combined with parent structure factors to calculate a 5-Å electron density map in order to define the approximate molecular envelope. An attempt to establish the correct molecular enantiomorph by calculation of parent Bijvoet difference Fourier maps using phases calculated from refined and inverted heavy atom derivative positions proved ambiguous (18). Consequently, parent maps were calculated by using phases from both refined and inverted sites and the highest peaks on these were compared with the parent Bijvoet difference Patterson map. This procedure gave a single consistent solution for the largest peak on one parent map, which on subsequent examination appeared to be centrally located in density corresponding to the expected size and shape of the heme prosthetic group. An electron density map incorporating data to 2.7-Å resolution was subsequently contoured on transparent plastic sheets to allow construction of a 2-cm/Å model in a Richards optical comparator (19).

The overall quality of the map obtained was reasonably good (Fig. 2), with the majority of the backbone chain course being fairly well defined as well as most of the internal amino acid side chains. Although some ambiguity exists in the backbone conformation around residues 32–36 and 65–70, we believe the overall molecular configuration presented here to be substantially correct. A more detailed description of this structure awaits the completion of the ongoing refinement at 2-Å resolution.

## RESULTS

The overall packing arrangement of the cytochrome  $c_{555}$  molecules in the unit cell is shown in Fig. 3. Fig. 4 is a ribbon

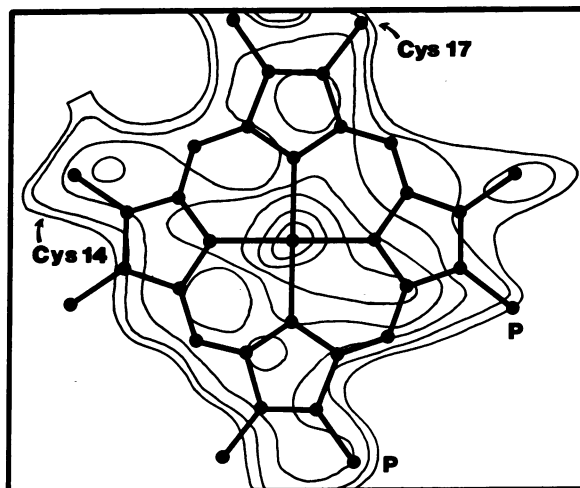


FIG. 2. Heme plane electron density at 2.7-Å resolution, contoured at 0.10, 0.16, 0.32, 0.48, 0.64, 0.80, and 0.90 of the positive dynamic range of the electron density map. Also shown are the locations of the covalent attachment points to the polypeptide chains (Cys 14 and 17) and positions of the heme propionic acid side chains (P).

representation of the molecule viewed from the direction of greatest heme exposure. Briefly, the molecule consists of an amino terminus  $\alpha$ -helix (residues 1–11) followed by residues furnishing the covalent thioether heme linkages (cysteine residues 14 and 17) and the fifth iron ligand (histidine-18). This is followed by a region forming the lower right quadrant of the structure (residues 20–40) which appears to be composed principally of type I hairpin bends. The chain subsequently ascends at the rear of the molecule and forms a single  $\alpha$ -helical turn (residues 42–46) prior to forming a large extended loop comprising the lower left side and bottom of the molecule (residues 47–59). The chain now ascends at the front of the molecule, with the sulfur atom of methionine-60 forming the sixth heme ligand, before extending rearward at the upper left of the molecule (residues 64–71). The chain is completed by a segment of  $\alpha$ -helix (residues 72–86) which descends diagonally at the rear of the molecule.

As is the case for other cytochrome  $c$  of known structure, the heme prosthetic group is essentially completely enveloped by the polypeptide chain, creating a hydrophobic heme environment allowing heme access only at a small region of the front of the molecule where one hydrophobic edge of the prosthetic group is exposed to solvent.

## DISCUSSION

As can be seen by comparison of the *C. thiosulfatophilum* structure (Fig. 4) with that of mitochondrial cytochrome  $c$  (Fig. 5), cytochrome  $c_{555}$  shares the majority of the features common to the larger high-potential cytochromes  $c$  thus far structurally investigated (1, 2). The principal structural difference that distinguishes cytochrome  $c_{555}$  results from an approximately 20-residue deletion in a region of the polypeptide chain that comprises the bottom of the larger molecules (see Fig. 5) and furnishes several residues that make hydrogen-bonded interactions with the buried heme propionate groups (1–3). Although it might be inferred that such a deletion would influence the extent of heme exposure in cytochrome  $c_{555}$ , it can be seen from Fig. 4 that the sequential deletion is structurally compensated for by an inward folding of a region of chain whose sequential analogue forms the left side of the larger molecules (Fig. 5). Thus, in fact, there appears to be little difference in the extent

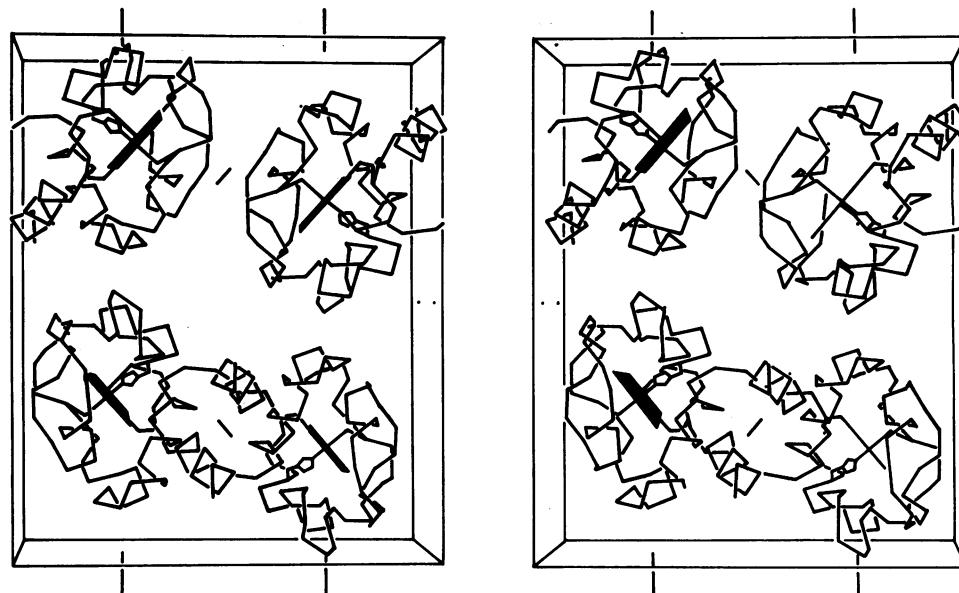


FIG. 3. Stereoscopic packing diagram of the cytochrome  $c_{555}$  unit cell. The  $a$  axis (48.3 Å) is horizontal, the  $c$  axis (60.1 Å) is vertical, and the  $b$  axis (24.5 Å) is perpendicular to the plane of the paper.

of heme exposure in cytochrome  $c_{555}$  and in the larger cytochromes  $c$ .

This last observation is of particular interest with regard to the proposals made by Kassner (20, 21) concerning the environmental factors responsible for the regulation of heme prosthetic group potential. Basically, it was suggested that the difficulty of accommodating a positive charge on the oxidized heme iron, relative to the uncharged reduced heme state, is dependent upon the dielectric constant of the local heme environment. Thus, heme prosthetic groups buried in the low-

dielectric hydrophobic interior of proteins (as they are in cytochromes  $c$ ) will be more stable in the uncharged reduced state and will consequently exhibit higher oxidoreduction potentials than otherwise identical prosthetic groups situated in an aqueous environment of high dielectric constant. Although this effect undoubtedly accounts for much of the observed oxidoreduction potential difference between aqueous heme com-

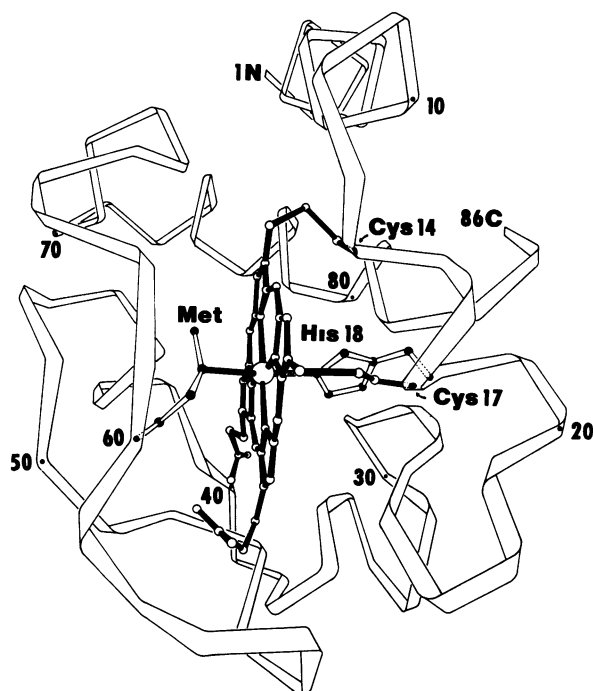


FIG. 4. Schematic representation of the *C. thiosulfatophilum* cytochrome  $c_{555}$  molecule. Axial heme iron ligands are furnished by an imidazole nitrogen of histidine-18 and the sulfur of methionine-60. See text for details. The view is similar to that of the upper right molecule in Fig. 3.

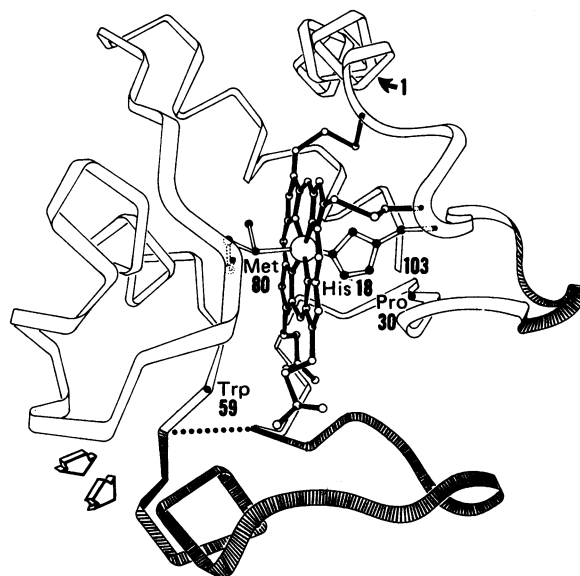


FIG. 5. Diagram of mitochondrial cytochrome  $c$  (1, 2), showing its structural relationship to *C. thiosulfatophilum* cytochrome  $c_{555}$  (Fig. 4). The principal structural difference between these molecules is a result of an approximately 20-residue structural deletion in the cytochrome  $c_{555}$  molecule in a region of the polypeptide chain (shown shaded), forming the bottom of the larger cytochrome  $c$  molecule. This deletion is structurally compensated in  $c_{555}$  by an inward folding of a sequentially analogous section of polypeptide chain comprising the outer left region of the cytochrome  $c$  structure, as indicated by the open arrows. In addition, cytochrome  $c_{555}$  differs by a short structural deletion at the right side of the cytochrome  $c$  molecule. Note that the views in Figs. 4 and 5 differ by a slight rotation about the horizontal axes of the molecules.

plexes and cytochromes *c*, it does not appear, insofar as heme exposure can be equated with heme hydrophobicity, that it can account for the observed potential differences between cytochrome *c*<sub>555</sub> and other cytochromes *c* of higher potential. It is further evident that the low oxidoreduction potential of cytochrome *c*<sub>555</sub> is not primarily related to its low molecular weight, because its overall size and molecular conformation are similar to those found for *Pseudomonas aeruginosa* cytochrome *c*<sub>551</sub> (R. E. Dickerson, personal communication) having a  $E_{m,7}$  of +285 mV, and it probably is similar to the algal cytochromes *f* (~85 residues,  $E_{m,7} \sim +330$ –+385 mV). Nevertheless, the possibility remains that some subtle differences in the nature or conformation of amino acid residues proximal to the heme may be responsible for the observed differences in oxidoreduction potentials in these proteins, although this has proved difficult to demonstrate for the known structures of mitochondrial cytochrome *c* and *Rhodospirillum* cytochrome *c*<sub>2</sub>, whose potentials differ by about 60 mV (1). Consequently it is hoped that a detailed structural comparison of the cytochrome *c*<sub>555</sub> molecule with cytochromes *c* of higher potential will yield some new insight into this problem.

From the evolutionary standpoint, the low oxidoreduction potential of cytochrome *c*<sub>555</sub> appears to reflect its functional role in an electron transport chain adapted to a strongly reducing environment (see Fig. 1), such as presumably existed prior to the emergence of photosynthetic organisms capable of splitting water. Nevertheless, as has been shown, this perhaps most primitive member of the cytochrome *c* family possesses the majority of the structural features characterizing cytochromes derived from higher organisms, despite the fact that there remains little trace of this ancestry in terms of sequence homology (1–3).

Thanks are due B. J. Errede, M. D. Kamen, and R. E. Dickerson who made information available prior to publication, to S. T. Freer, L. Reed, S. Jordan, and P. Weber, who assisted in the implementation of the computer programs required for this study, and to E. M. Stonebraker

for his expert mechanical contributions. This work was supported by the National Science Foundation (BMS75-06558), the National Institutes of Health (GM21534), and the University of Arizona Computer Center.

1. Salemme, F. R. (1977) *Annu. Rev. Biochem.* **46**, 299–329.
2. Dickerson, R. E. & Timkovich, R. (1975), "Oxidation/reduction," in *The Enzymes*, ed. Boyer, P. D. Vol. XL, (Academic Press, New York) Vol. 40, Part A, pp. 397–497.
3. Ambler, R. P. (1974) *Syst. Zool.* **22**, 554–565.
4. Kamen, M. D. & Vernon, L. P. (1954) *J. Bacteriol.* **67**, 617–618.
5. Gibson, J. (1961) *Biochem. J.* **79**, 151–158.
6. Yamanaka, T. & Okunuki, K. (1968) *J. Biochem. (Tokyo)* **63**, 341–346.
7. Meyer, T. E., Bartsch, R. G., Cusanovich, M. A. & Mathewson, J. H. (1968) *Biochim. Biophys. Acta* **153**, 854–861.
8. Van Beeumen, J., Ambler, R. P., Meyer, T. E., Kamen, M. D., Olson, J. M. & Shaw, E. K. (1976) *Biochem. J.* **159**, 757–774.
9. Kusai, K. & Yamanaka, T. (1973) *Biochim. Biophys. Acta.* **325**, 304–314.
10. Kamen, M. D., Dus, K. M., Flatmark, T. & de Klerk, H. (1971) in *Treatise on Electron and Coupled Energy Transfer in Biological Systems*, eds. King, T. E. & Klingenberg, M. (Marcel Dekker, New York); pp. 243–324.
11. Davis, K. A., Hatefi, Y., Salemme, F. R. & Kamen, M. D. (1972) *Biochem. Biophys. Res. Commun.* **49**, 1329–1335.
12. Errede, B. J. (1977) Dissertation, University of California, San Diego, CA.
13. Errede, B. J. & Kamen, M. D. (1977) *Biochemistry*, in press.
14. Salemme, F. R. (1972) *Arch. Biochem. Biophys.* **151**, 533–539.
15. Salemme, F. R., Freer, S. T., Xuong, N. H., Alden, R. A. & Kraut, J. (1973) *J. Biol. Chem.* **248**, 3910–3921.
16. Furnas, T. C. (1967) *Single Crystal Orienter Instruction Manual* (General Electric Co., Milwaukee, WI).
17. Matthews, B. W. (1966) *Acta Crystallogr.* **20**, 82–86.
18. Kraut, J. (1968) *J. Mol. Biol.* **35**, 511–512.
19. Richards, F. M. (1968) *J. Mol. Biol.* **37**, 225–230.
20. Kassner, R. J. (1973) *J. Am. Chem. Soc.* **95**, 2674–2677.
21. Kassner, R. J. (1972) *Proc. Natl. Acad. Sci. USA* **69**, 2263–2267.